3-28-2004

Observations of Solar Cyclical Variations in Geocoronal Hα Column Emission Intensities

S. M. Nossal
University of Wisconsin-Madison

F. L. Roesler
University of Wisconsin-Madison

E. J. Mierkiewicz
University of Wisconsin - Madison, mierkiee@erau.edu

R. J. Reynolds
University of Wisconsin-Madison

Observations of solar cyclical variations in geocoronal Hα column emission intensities

S. M. Nossal,[1] F. L. Roesler,[1] E. J. Mierkiewicz,[1] and R. J. Reynolds[2]

Received 26 September 2003; revised 30 January 2004; accepted 9 February 2004; published 20 March 2004.

[1] Observations of thermospheric + exospheric Hα column emissions by the Wisconsin Hα Mapper (WHAM) Fabry-Perot (Kitt Peak, Arizona) over the 1997–2001 rise in solar cycle 23 show a statistically significant solar cyclical variation. The higher signal-to-noise WHAM observations corroborate suggestions of a solar cycle trend in the Hα emissions seen in Wisconsin observations over solar cycle 22. Here we compare WHAM 1997 and 2000–2001 winter solstice geocoronal Hα observations toward regions of the sky with low galactic emission. The observed variation in geocoronal hydrogen column emission intensities over the solar cycle is small compared with variations in hydrogen exobase densities. Higher Hα emissions are seen during solar maximum periods of the solar cycle. At a mid range shadow altitude (3000 km), WHAM geocoronal Hα intensities are about 45% higher during solar maximum than during solar minimum. *INDEX TERMS:* 0310 Atmospheric Composition and Structure: Airglow and aurora; 0355 Atmospheric Composition and Structure: Thermosphere—composition and chemistry; 0394 Atmospheric Composition and Structure: Instruments and techniques; 1650 Global Change: Solar variability. **Citation:** Nossal, S. M., F. L. Roesler, E. J. Mierkiewicz, and R. J. Reynolds (2004), Observations of solar cyclical variations in geocoronal Hα column emission intensities, *Geophys. Res. Lett.*, *31*, L06110, doi:10.1029/2003GL018729.

1. Introduction

[2] Upward fluxes of hydrogen-containing molecules such as methane, water vapor, and molecular hydrogen are the primary sources of hydrogenous species in the middle and upper atmosphere. Geocoronal hydrogen is the byproduct of middle and upper atmospheric chemical, photolysis, and charge exchange reactions involving hydrogenous species such as H_2O, CH_4, H_2, OH, CH_2O and H^+ [see, e.g., *Brasseur and Solomon*, 1986]. Atomic hydrogen spans the thermosphere and exosphere, becoming increasingly dominant with altitude. Due to its long orbital trajectories, upper atmospheric hydrogen is more globally mixed compared with its hydrogenous source species below.

[3] Ground-based remote sensing of the very faint fluorescence emissions from atomic hydrogen [Hα (6563Å ~ 1–10 Rayleighs), and, more recently, Hβ (4861Å ~ 0.25–1 Rayleigh)] is one of the primary diagnostics for studying the neutral upper atmosphere. The Fabry-Perot Spectrometer is particularly advantageous for making observations of faint, diffuse sources such as the geocorona due to the instrument's simultaneous high spectral resolution and high throughput.

[4] The thermospheric+exospheric Hα emission is primarily excited by the line center portion of the solar Lyman-β (1026Å) flux. Most of the Hα emission thus comes from above the Earth's shadow, the height of which can be used to determine, to first order, the base of the column of Hα emission. As such, the Hα emission intensity is dependent upon the hydrogen density profile, the solar excitation flux, and the observational viewing geometry. The Hα column emission intensity observed by the Fabry-Perot is a measurement of the integrated volume emission rate along the observational line-of-sight, with the peak in the emission rate arising from just above the Earth's shadow.

[5] This paper investigates the influence of solar cyclical variability upon thermospheric+exospheric hydrogen Hα emissions via analysis of winter solstice, low galactic emission region observations made by the Wisconsin Hα Mapper Fabry-Perot (WHAM) from the Kitt Peak Observatory, near Tucson, Arizona (LAT 31.98°; LON −111.60°).

2. Observations

[6] Long term comparisons of thermospheric+exospheric Hα emissions require a stable calibration source, cross-calibrated and well-understood instrumentation, reproducible observing conditions, separation of the terrestrial from the galactic emission line, and consistent data analysis, accounting for differences in viewing geometry.

[7] The ground-based Wisconsin Hα Mapper Fabry-Perot is a remotely operated, semi-automated, 15 cm double-etalon Fabry-Perot. Using the CCD-based (charge coupled device camera) annular summing technique [*Coakley et al.*, 1996], WHAM has acquired approximately 38,000 Hα spectra since it began observing in 1997. WHAM's resolving power [~25,000] is sufficient for separation of the terrestrial emission from the Doppler-shifted galactic line and for retrieval of the Hα emission intensity.

[8] WHAM is used primarily for making astronomical observations of interstellar medium emissions, including an all-sky survey of interstellar Hα emissions [*Reynolds*, 1997; *Haffner et al.*, 2003]. The terrestrial spectra present in these observations comprise a rich resource of observations in multiple viewing geometries for studying thermospheric+exospheric atomic hydrogen Hα emissions. In

[1]Department of Physics, University of Wisconsin, Madison, Wisconsin, USA.
[2]Department of Astronomy, University of Wisconsin, Madison, Wisconsin, USA.

0094-8276/04/2003GL018729$05.00

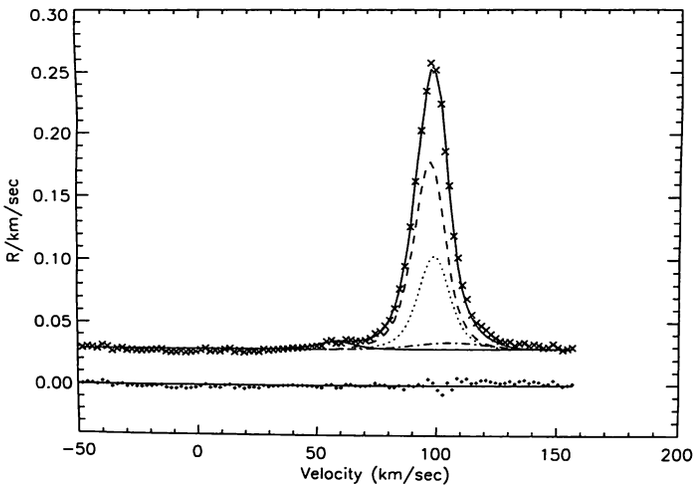

Figure 1. Sample WHAM Hα nightsky spectrum in a region of low galactic emission (~30 second exposure). Spectral displacement is expressed in velocity units. Zero velocity is placed at an arbitrary location. The centroid of the two component fit to the geocoronal line is located at 96.8 km/sec and its intensity is 4.1 Rayleighs (R). The fit in Figure 1 also includes the galactic emission (0.20 R) at 105 km/sec and a faint atmospheric emission (0.13 R) at 57.5 km/sec (see text and *Hausen et al.* [2002]).

addition, WHAM also makes observations in directions specifically designed for geocoronal studies.

[9] The observations presented in this paper were limited to those WHAM observations taken during winter solstice conditions and in observing directions pointed toward low galactic emission [less than about 0.25 Rayleigh at Hα] regions of the sky. Most were pointed toward the Lockman window [right ascension (RA) 10.90°, declination (DEC) 57.93°], with some also pointed toward other regions of low galactic emission [(RA 10.38°, DEC 50.24°), (RA 10.81°, DEC 37.57°)] [*Hausen et al.*, 2002]. Such observations minimize uncertainty due to blending between the galactic and terrestrial Hα emission lines. The winter solstice typically offers the best sky conditions for observations, as well as longer nights. To insure consistent observing conditions, we only use observations taken during dark moon and clear sky conditions. Low galactic emission region observations, such as those presented in this paper, are routinely taken as standard observations during almost all nights of WHAM observations.

3. Calibration

[10] The absolute intensity of the thermospheric+exospheric Hα column emission is calibrated through comparisons with Hα emissions from standard astronomical nebular calibration sources, all of which have been tied to the North American Nebula (NAN). Nebular calibration is internally consistent and is used for calibrating all of the Wisconsin-based atmospheric, planetary, and astronomical hydrogen Hα observations. Nebular calibration offers long term stability and like the geocorona, nebulae are spatially extended line rather than continuum emission sources. The use of nebular calibration minimizes uncertainty due to atmospheric extinction corrections since both the geocoronal hydrogen and the nebular calibration sources are outside of the Earth's atmosphere. Corrections are made for differences in atmospheric extinction due to differences in slant path between the observational and calibration look directions.

[11] The absolute intensity calibration of the WHAM observations has been tied to a 1° patch (centered at right ascension 20h 57m 59s and declinaton +44d 34′ 50″) of the North American Nebula whose intensity is 800 R ± 10%. There is about a 5% uncertainty in the relative calibration due to night to night variability in the transmittance of the atmosphere. The North American Nebula has been calibrated for Hα using standard stars [*Scherb*, 1981] and has also been checked against a blackbody source [*Nossal*, 1994]. The accuracy of this calibration has also been corroborated with a comparison to the Southern Hα Sky Survey Atlas [*Gaustad et al.*, 2001].

4. Data Analysis

[12] After processing the CCD image of the Fabry-Perot interference pattern to remove the bias, dark counts, and hot pixels, ring summing was performed to convert the annular interference pattern to a line profile. The spectrum was divided by a white light flat field to compensate for vignetting within the instrument and pixel-to-pixel variation on the CCD chip [*Coakley et al.*, 1996; *Haffner et al.*, 2003]. The exposure times for observations presented in this paper ranged from 30 seconds to 600 seconds. The resolving power of the WHAM Fabry-Perot is too low to resolve accurately the geocoronal Hα emission line width; higher resolution observations have shown the line width to be about 6–8 km/sec [see, e.g., *Nossal et al.*, 1998; *Mierkiewicz*, 2002].

[13] Figure 1 shows a sample geocoronal Hα emission spectrum used in the low galactic emission region study presented in this paper. The observation was made on March 13, 1997 using an exposure time of 30 seconds. The emission line intensity was 4.1 Rayleighs. Spectral displacements are expressed here in velocity units (an interval of 1 km/sec corresponds to 0.0219 Å or 0.0508 cm^{-1} at Hα) with the "zero" velocity point placed at an arbitrary location.

[14] The geocoronal Hα emission was fitted using a two Gaussian model representing the two dominant fine structure transitions ($3^2P_{3/2}$ to $2^2S_{1/2}$; $3^2P_{1/2}$ to $2^2S_{1/2}$; centroid wavelength in air of 6562.741 Å) contributing to the geocoronal Hα emission. The separation of the line centers of the two Gaussians was fixed to be that of the spectral spacing between these two fine structure components [2.133 km/sec] and the ratio of their areas was fixed as 2:1, corresponding to the quantum mechanical ratio of the transition probabilities of the two dominant fine structure emissions [see, e.g., *Nossal et al.*, 1998]. The spectral location of the doublet, its total area, and the intensity of the background continuum were all free parameters. This two component geocoronal Hα emission model was convolved with the instrumental profile and then fit to the geocoronal Hα emission line profile. The model was adjusted subject to the above constraints to produce a least squares, best-fit to the data using the voigt-fit code of R. C. Woodward (personal communication, 2003).

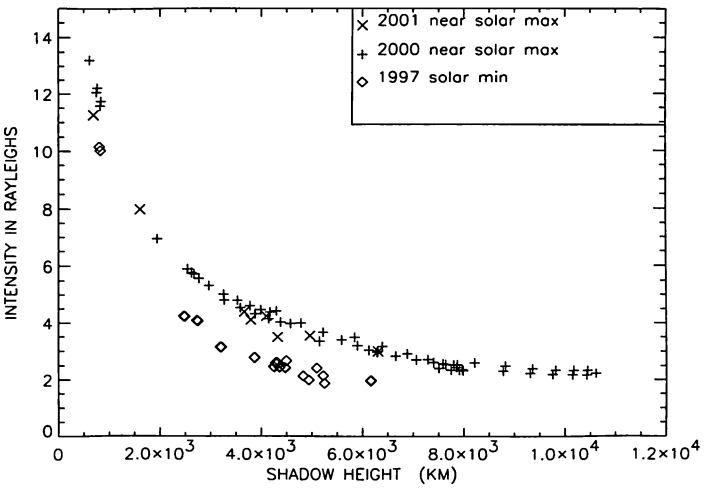

Figure 2. Winter solstice WHAM thermospheric+exospheric Hα column emission intensities. All of these observations were made pointing toward regions of the sky with low galactic emission. Intensities have been plotted versus the altitude of the Earth's shadow. The data included on this plot came from 18 nights of observations between December and the spring equinox (ten nights from 1997, three nights from 1999-2000, and five nights from 2001).

[15] Explicit fitting of the geocoronal Hα fine structure emission components arising due to cascade excitation [see *Meier*, 1995; *Nossal et al.*, 1998, and references therein] has not been included in the fits to the data presented in this paper because the resolution of the WHAM instrument is too low to resolve the geocoronal line profile. The retrieved geocoronal intensities include the cascade excitation which is estimated to be 5 ± 3% of the total intensity based upon recent observations by *Mierkiewicz* [2002] and revised estimates by R. R. Meier (personal communication, 2004).

[16] In addition to the two component fit to the geocoronal line (centroid at 96.8 km/sec), the total fit in Figure 1 also includes fits to the galactic emission centered at 105 km/sec (0.20 Rayleighs) and to a faint (0.13 Rayleigh) atmospheric emission line centered at 57.5 km/sec (6561.9 Å, air wavelength), likely from the $N2^+$ Meinel (6, 2) band [see, e.g., *Strickland et al.*, 1999]. These emissions were fit with parameters fixed according to those measured by *Hausen et al.* [2002]. This example spectrum represents a case with near maximum overlap between the geocoronal and Lockman window galactic emissions. Greater doppler shifts between the two lines results in less overlap. For the spectrum of Figure 1, the geocoronal Hα column emission intensity retrieved when the Lockman window galactic emission is included in the fit differs by less than 4% from that retrieved when the galactic emission is not fit. Detailed fitting of the galactic emission has not been done for the data presented in this paper because of the faintness of galactic emission in these regions of the sky.

[17] The absolute intensity of the geocoronal Hα emission is retrieved by comparing its integrated area with that from the nebular calibration source. The difference in atmospheric extinction between the two observations is then accounted for from their difference in slant path, using the measured zenith transmission of 0.92 ± 3% for a clear night on Kitt Peak [*Haffner et al.*, 2003].

[18] Figure 2 displays thermospheric+exospheric Hα column emission intensities as a function of shadow altitude for changing solar conditions. The shadow altitude is determined by the optical depth of solar Lymanβ radiation and the observational look direction. Solar Lymanβ is fully absorbed by atmospheric O_2 below 102 km. Thus, for Lymanβ excitation, the Earth's shadow forms a cylinder with a radius that is 102 km greater than that of the Earth. The shadow altitude is the viewing geometry parameter with the greatest influence on the column geocoronal Hα emission intensity. Small changes in intensity related to observational zenith angle and azimuth variations for a constant shadow height can also be detected [*Nossal et al.*, 2001].

[19] In Figure 2, the 1997 observations were taken during solar minimum conditions and are indicated by the diamond symbol. The 2000 and 2001 observations were taken during near solar maximum conditions and are represented by the "+" and "x" symbols, respectively. The data included on this plot came from 18 nights of observations between December and the spring equinox. The 1997 points are from ten nights, the 1999–2000 winter solstice data are from three nights, and the 2001 data are from five nights of observations. The F10.7 index ranged from 69–76 for the solar minimum data and from 134–163 for the near solar maximum data. We observe higher intensities during the solar maximum periods of solar cycle 23. The increase in geocoronal Hα intensity observed by WHAM between solar minimum and solar maximum conditions depends upon viewing geometry. For example, at the mid range shadow altitude of 3000 km, WHAM geocoronal Hα column intensities are about 45% higher during solar maximum conditions.

[20] The thermospheric+exospheric Hα column emission intensities displayed in Figure 2 have not been corrected for scattering in the troposphere. When corrections are made to these data using the tropospheric scattering code of *Leen* [1979; *Shih et al.*, 1985], the intensities are lowered by 14–26%, depending upon the viewing geometry. The conclusions of this paper are unchanged because the corrections apply both to solar minimum and maximum conditions. For example, at a midrange shadow altitude of 3000 km, the geocoronal Hα column emission intensity is still about 45% higher during solar maximum conditions than during solar minimum conditions when the intensities are corrected for tropospheric scattering using the Leen code. We have chosen to report only the primary measurements because we recognize the need for an improved scattering code for the higher precision measurements. We are in the process of refining the tropospheric scattering code.

5. Discussion

[21] The higher signal-to-noise WHAM observations over the 1997–2001 rise in the solar cycle corroborate suggestions of a solar cycle trend in the Hα emissions seen in Wisconsin observations taken over the previous solar cycle (cycle 22) [*Nossal et al.*, 1993]. The Wisconsin-based observations over solar cycle 22 also measured higher geocoronal Hα intensities during solar maximum periods; however past data were deemed to be of insufficient precision to make the variation statistically significant.

Collectively, the mid latitude observations by Wisconsin observers [*Nossal et al.*, 1993, 2001; *Mierkiewicz*, 2002, and references therein] now span two solar cycles.

[22] The observed variation in the thermospheric+exospheric Hα column emission intensity over the solar cycle is small compared with the variations in the hydrogen exobase density. The Mass Spectrometer Incoherent Scatter-90 (MSIS-90) empirical model of the middle and upper atmosphere [*Hedin*, 1991] indicates a variation in hydrogen density at 500 km of a factor of about nine over the solar cycle, with higher densities during solar minimum periods. Empirical solar EUV models [*Lean et al.*, 2003] predict that the line integrated solar Lyman-β flux varies by a factor of at most two over the solar cycle, with higher fluxes during solar maximum periods. Detailed modeling is needed to retrieve hydrogen column abundance information from the Hα emission observations [*Bishop*, 1999]. Case studies indicate that the hydrogen column abundance can be retrieved via forward modeling analysis [*Bishop et al.*, 2001] with studies currently in progress to assess the sensitivity of retrievals to radiative transport forward modeling parameters [*Bishop et al.*, 2004].

[23] The mid latitude solar cyclical variation in the geocoronal Hα emission observed by WHAM and previous Wisconsin-based Fabry-Perot instruments differs from that seen at the lower latitude Arecibo Observatory by *Kerr et al.* [2001]. Intensities seen in the Arecibo data are typically 50% *greater* at solar *minimum* than under solar maximum conditions for solar depression angles between 15° and 35° with no evident solar cycle variation in intensity seen for solar depression angles above about 40° (corresponding to a shadow altitude of about 2000 km) [*Kerr et al.*, 2001]. The solar cycle variation observed at Arecibo is opposite to that which we see at the mid latitude Kitt Peak and Wisconsin sites of *higher* column emission intensity during solar *maximum* periods.

[24] Understanding the influence of solar cyclical variation on the Earth's upper atmosphere is important for determining the present basic state of this region, as well as for distinguishing between natural variability and possible observational signatures of climate change in the upper atmosphere [*Roble*, 1995]. The high signal-to-noise, and consistent calibration of the WHAM geocoronal Hα emission observations facilitate their use as benchmark data for comparisons with past and future data sets.

[25] **Acknowledgments.** We thank Matt Haffner, Steve Tufte, Nicole Hausen, Greg Madsen, and Robert Benjamin for the WHAM observations and for helpful discussions about the data. We are also very grateful to R. Carey Woodward and Jeff Percival for assistance with writing and applying data analysis tools. We are indebted to James Bishop for his collaboration and insights concerning analysis, theory, modeling, and other issues pertaining to the geocorona. We also thank John Harlander and Frank Scherb for their long term contributions to our geocoronal research program. We appreciate the reviewer's helpful comments. This research was supported by the National Science Foundation grants ATM-0003166 and AST-9619424.

References

Bishop, J. (1999), Transport of resonant atomic hydrogen emissions in the thermosphere and geocorona: Model description and applications, *J. Quant. Spectrosc. Radiat. Transfer*, *61*, 473–491.

Bishop, J., J. Harlander, S. Nossal, and F. L. Roesler (2001), Analysis of Balmer α intensity measurements near solar minimum, *J. Atmos. Sol. Terr. Phys.*, *63*, 341–353.

Bishop, J., E. J. Mierkiewicz, F. L. Roesler, J. F. Gomez, and C. Morales (2004), Data-model comparison search analysis of coincident PBO Balmer α, EURD Lyman β geocoronal measurements from March 2000, *J. Geophys. Res.*, doi:10.1029/2003JA010165, accepted.

Brasseur, G., and S. Solomon (1986), *Aeronomy of the Middle Atmosphere*, D. Reidel, Norwell, Mass.

Coakley, M. M., F. L. Roesler, R. J. Reynolds, and S. Nossal (1996), Fabry-Perot/CCD annular summing spectroscopy: Study and implemenation for aeronomy applications, *Appl. Opt.*, *35*, 6479–6493.

Gaustad, J. E., P. R. McCullough, W. Rosing, and D. Van Buren (2001), A robotic wide-angle H-alpha survey of the southern sky, *Publ. Astron. Soc. Pac.*, *113*, 1326–1348.

Haffner, L. M., R. J. Reynolds, S. L. Tufte, G. J. Madsen, K. P. Jaehnig, and J. W. Percival (2003), The Wisconsin H-alpha mapper northern sky survey, *Astrophys. J.*, *149*, 405–422.

Hausen, N. R., R. J. Reynolds, L. M. Haffner, and S. L. Tufte (2002), Interstellar Hα line profiles toward HD 93521 and the Lockman window, *Astrophys. J.*, *565*, 1060–1068.

Hedin, A. E. (1991), Extension of the MSIS thermosphere model into the middle and lower atmosphere, *J. Geophys. Res.*, *96*, 1159–1172.

Kerr, R. B., et al. (2001), Periodic variations of geocoronal Balmer-α brightness due to solar driven exospheric abundance variations, *J. Geophys. Res.*, *106*, 28,797–28,817.

Lean, J., H. P. Warren, J. T. Mariska, and J. Bishop (2003), A new model of solar EUV irradiance variability: 2. Comparisons with empirical models and observations and implications for space weather, *J. Geophys. Res.*, *108*(A2), 1059, doi:10.1029/2001JA009238.

Leen, T. (1979), Application of radiative transfer theory to photometric studies of astronomical objects, M.S. thesis, Univ. of Wis., Madison.

Meier, R. R. (1995), Solar Lyman-series line profiles and atomic hydrogen excitation rates, *Astrophys. J.*, *452*, 462–471.

Mierkiewicz, E. J. (2002), Fabry-Perot observations of the hydrogen geocorona, Ph.D. thesis, Univ. of Wis., Madison.

Nossal, S. (1994), Fabry-Perot observations of geocoronal hydrogen Balmer-α emissons, Ph.D. thesis, Univ. of Wis., Madison.

Nossal, S., R. J. Reynolds, F. L. Roesler, and F. Scherb (1993), Solar cycle variations of geocoronal Balmer α emission, *J. Geophys. Res.*, *98*, 3669–3676.

Nossal, S., F. L. Roesler, and M. M. Coakley (1998), Cascade excitation in the geocoronal hydrogen Balmer α line, *J. Geophys. Res.*, *103*, 381–390.

Nossal, S., F. L. Roesler, R. J. Reynolds, M. Haffner, S. Tufte, J. Bishop, and J. Percival (2001), Geocoronal Balmer α intensity measurements using the WHAM Fabry-Perot facility, *J. Geophys. Res.*, *106*, 5605–5616.

Reynolds, R. J. (1997), Ionizing the galaxy, *Science*, *277*, 1446–1447.

Roble, R. G. (1995), Major greenhouse cooling (yes, cooling): The upper-atmosphere response to increased CO_2, *U.S. Natl. Rep. Int. Union Geod. Geophys. 1991–1994, Rev. Geophys.*, *33*, 539–546.

Scherb, F. (1981), Hydrogen production rates from ground-based Fabry-Perot observations of comet Kohoutek, *Astrophys. J.*, *243*, 644–650.

Shih, P., F. L. Roesler, and F. Scherb (1985), Intensity variations of geocoronal Balmer alpha emission: 1. Observational results, *J. Geophys. Res.*, *90*, 477–490.

Strickland, D. J., J. Bishop, J. S. Evans, T. Majeed, P. M. Shen, R. J. Cox, R. Link, and R. E. Huffman (1999), Atmospheric ultraviolet radiance integrated code (AURIC): Theory, software architecture, inputs and selected results, *J. Quant. Spectrosc. Radiat. Transfer*, *62*, 689–742.

E. J. Mierkiewicz, S. M. Nossal, and F. L. Roesler, Department of Physics, University of Wisconsin, 1150 University Ave., Madison, WI 53706, USA. (nossal@wisp.physics.wisc.edu)

R. J. Reynolds, Department of Astronomy, University of Wisconsin, Madison, Wisconsin, USA.